Science Advances
AAAS

advances.sciencemag.org/cgi/content/full/sciadv.abe5575/DC1

Supplementary Materials for

Conformational dynamics of SARS-CoV-2 trimeric spike glycoprotein in complex with receptor ACE2 revealed by cryo-EM

Cong Xu, Yanxing Wang, Caixuan Liu, Chao Zhang, Wenyu Han, Xiaoyu Hong, Yifan Wang, Qin Hong, Shutian Wang, Qiaoyu Zhao, Yalei Wang, Yong Yang, Kaijian Chen, Wei Zheng, Liangliang Kong, Fangfang Wang, Qinyu Zuo, Zhong Huang*, Yao Cong*

*Corresponding author. Email: cong@sibcb.ac.cn (Y.C) and huangzhong@ips.ac.cn (Z.H.)

Published 4 December 2020, *Sci. Adv.* **6**, eabe5575 (2020)
DOI: 10.1126/sciadv.abe5575

This PDF file includes:

Other Supplementary Material for this manuscript includes the following:

(available at advances.sciencemag.org/cgi/content/full/sciadv.abe5575/DC1)

SUPPLEMENTARY MATERIALS

Supplementary Figures and Legends

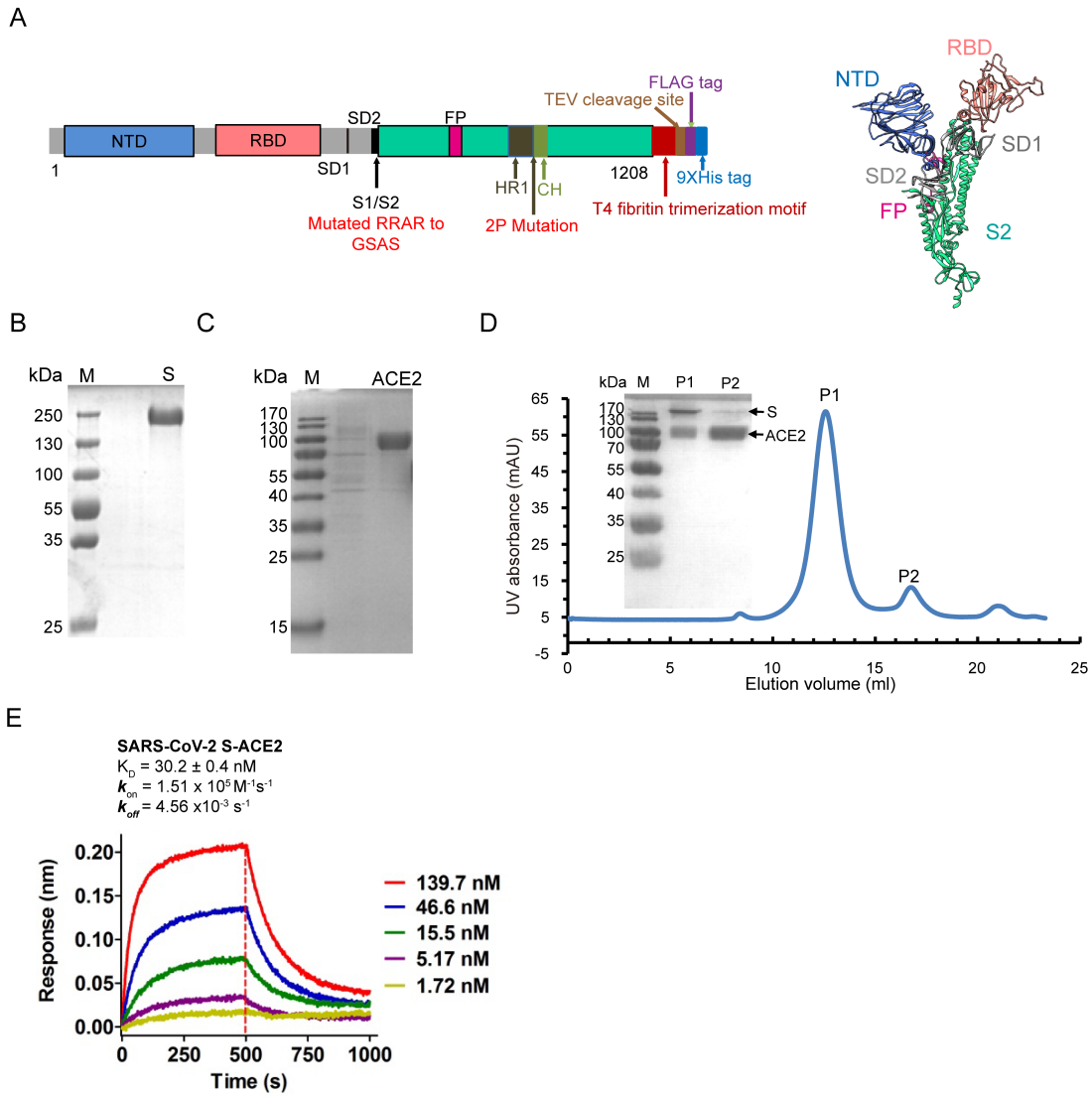

Fig. S1. Purification of SARS-CoV-2 S ectodomain, human ACE2 PD domain, and S-ACE2 complex. (A) Schematic diagram of SARS-CoV-2 S organization in this study. S1/S2 protease cleavage site (S1/S2), N-terminal domain (NTD), receptor-binding domain (RBD), fusion peptide (FP), heptad repeat 1 (HR1), and central helix (CH) are labeled. (B-C) SDS-PAGE analysis of the purified S protein (B) and ACE2 (C). (D) Size-exclusion chromatogram and SDS-PAGE analysis of the formed S-ACE2 complex. (E) Measurement of the binding affinity and kinetics of S trimer and ACE2 using bio-layer interferometry (BLI).

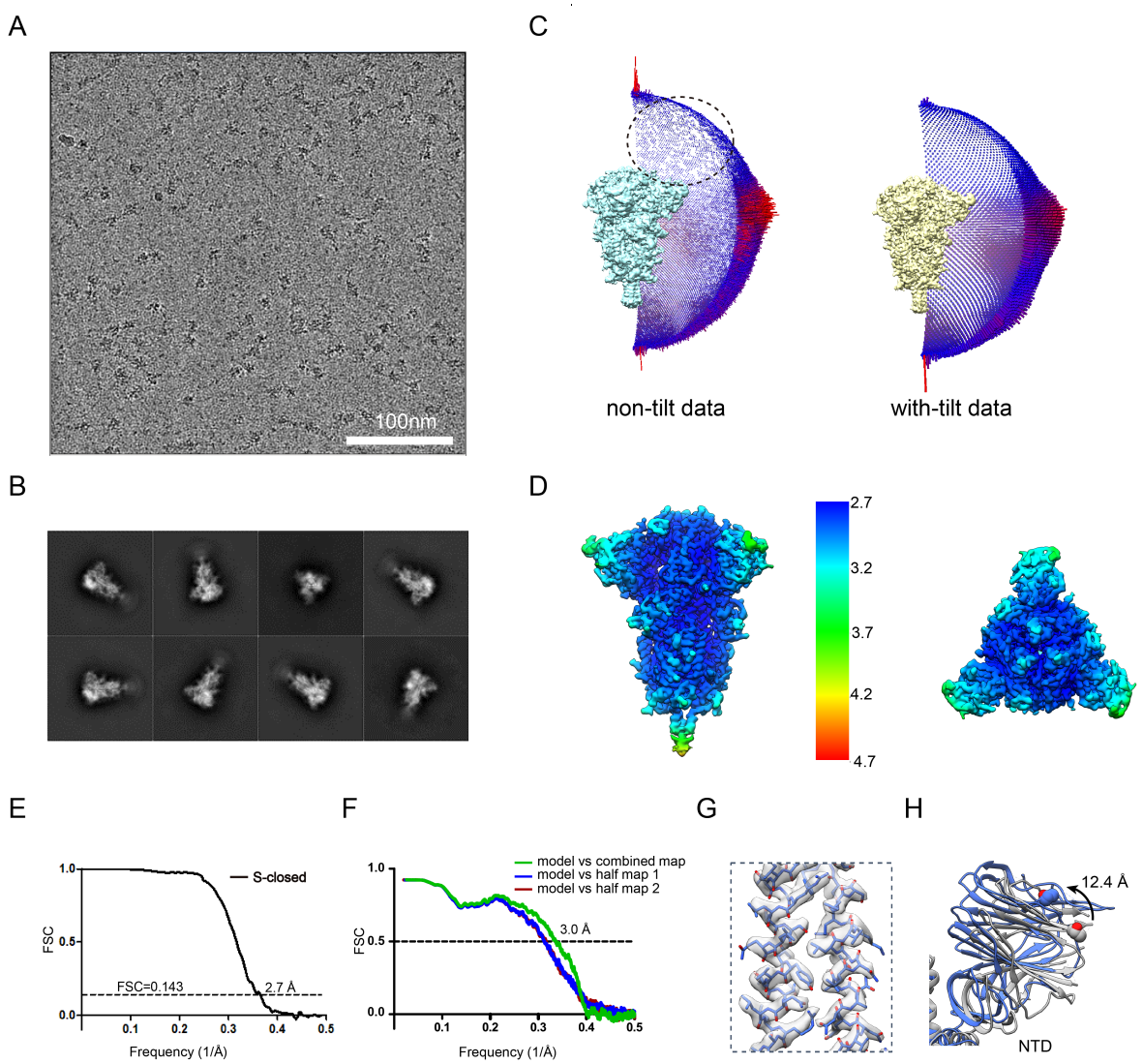

Fig. S2. Cryo-EM analysis of the SARS-CoV-2 S trimer in the tightly closed state. (A) Representative cryo-EM image of the SARS-CoV-2 S trimer. (B) Reference-free 2D class averages of the S trimer. (C) Euler angular distribution of 3D reconstructions before and after adding tilt data, with the dotted circle indicating the sparsely distributed tilted top views in the non-tilt data. (D-E) Local resolution evaluation (D) and resolution assessment of our S-closed cryo-EM map by Fourier shell correlation (FSC) at 0.143 criterion (E). (F) The model vs map FSC curve at 0.5 criterion for S-closed (green). FSC curves between the refined atomic model and half-map 1 that the model refined against (blue), and between the refined atomic model and half-map 2 (dark red); differences between the two curves are small, indicating the refinement of the atomic coordinates did not suffer from overfitting. (G) Close up view of the model-map fitting in S2 subunit. (H) Compared with the recent structure of SARS-CoV-2 S in closed state (gray, 6VXX), our S-closed structure (blue) showed a slight inward tilt leading the peripheral edge of NTD exhibiting a 12.4 Å inward movement (for the Cα of T124).

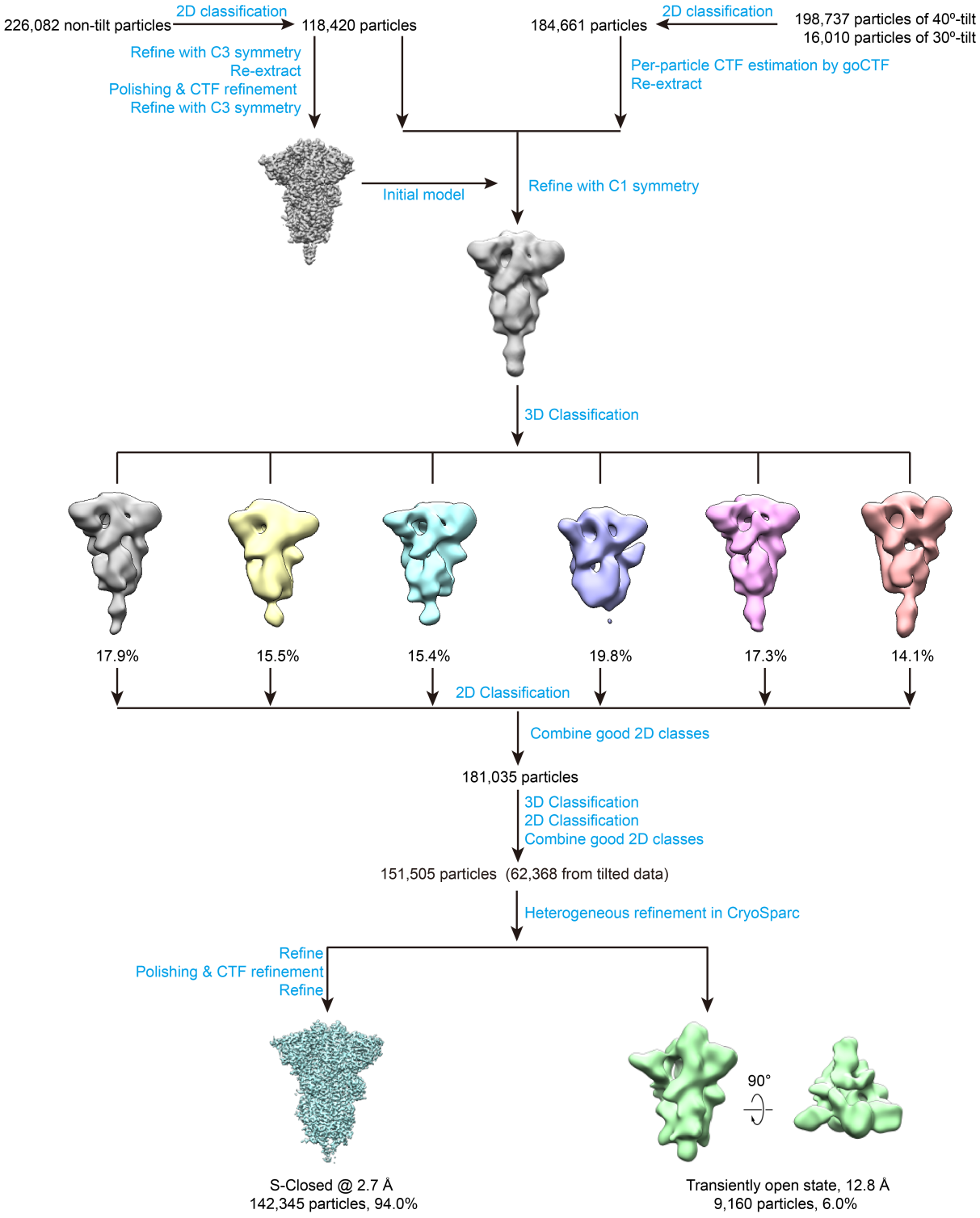

Fig. S3. Cryo-EM data processing procedure for SARS-CoV-2 S trimer.

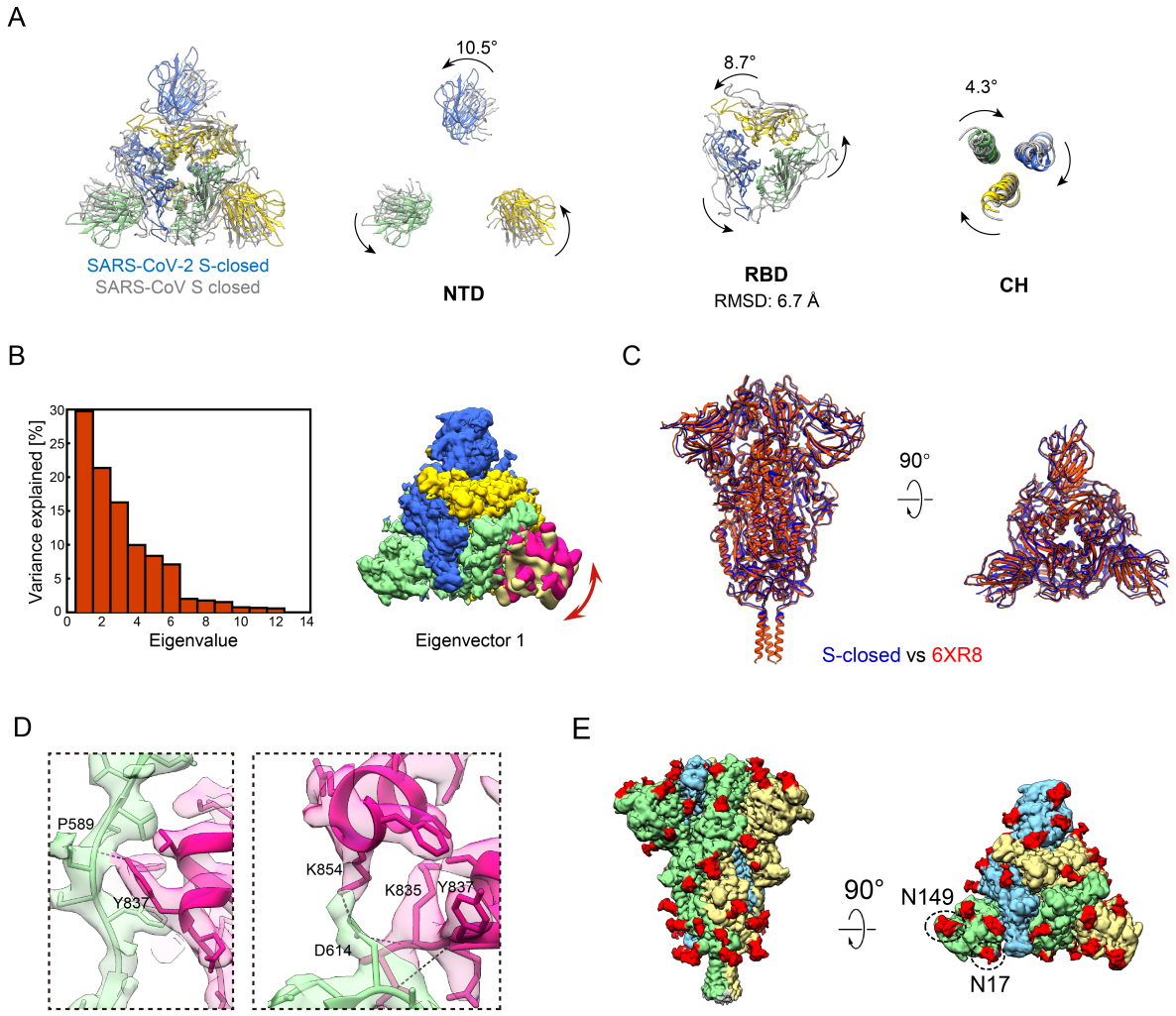

Fig. S4. Structural analysis of the SARS-CoV-2 S-closed state. (A) Top view of the overlaid structures between our SARS-CoV-2 S-closed and the SARS-CoV S closed structure (PDB: 5XLR) and zoom in views of the overlaid structures in NTD, RBD, CH domains. (B) Multi-body refinement and PCA analysis of the NTD region on S-closed state. Left, the contribution of all eigenvectors to the motion in the S trimer, with Eigenvector 1 contributes ~30% of the movement of the S trimer. Right, top view of the map showing the NTD in-plane swing motion (indicated by dark red arrow) of Eigenvector 1. (C) Structural comparison between our S-closed structure (blue) and the wild-type S trimer prefusion structure (PDB: 6XR8, orange). The two structures are in similar conformation. (D) Detailed density of FP and critical interactions including some salt-bridge/H-bond formed between FP and surrounding residues. FP is colored in deep pink, and SD2 from adjacent protomer in light green. (E) N-linked glycans resolved in our S-closed cryo-EM map, with the densities corresponding to glycans colored in red.

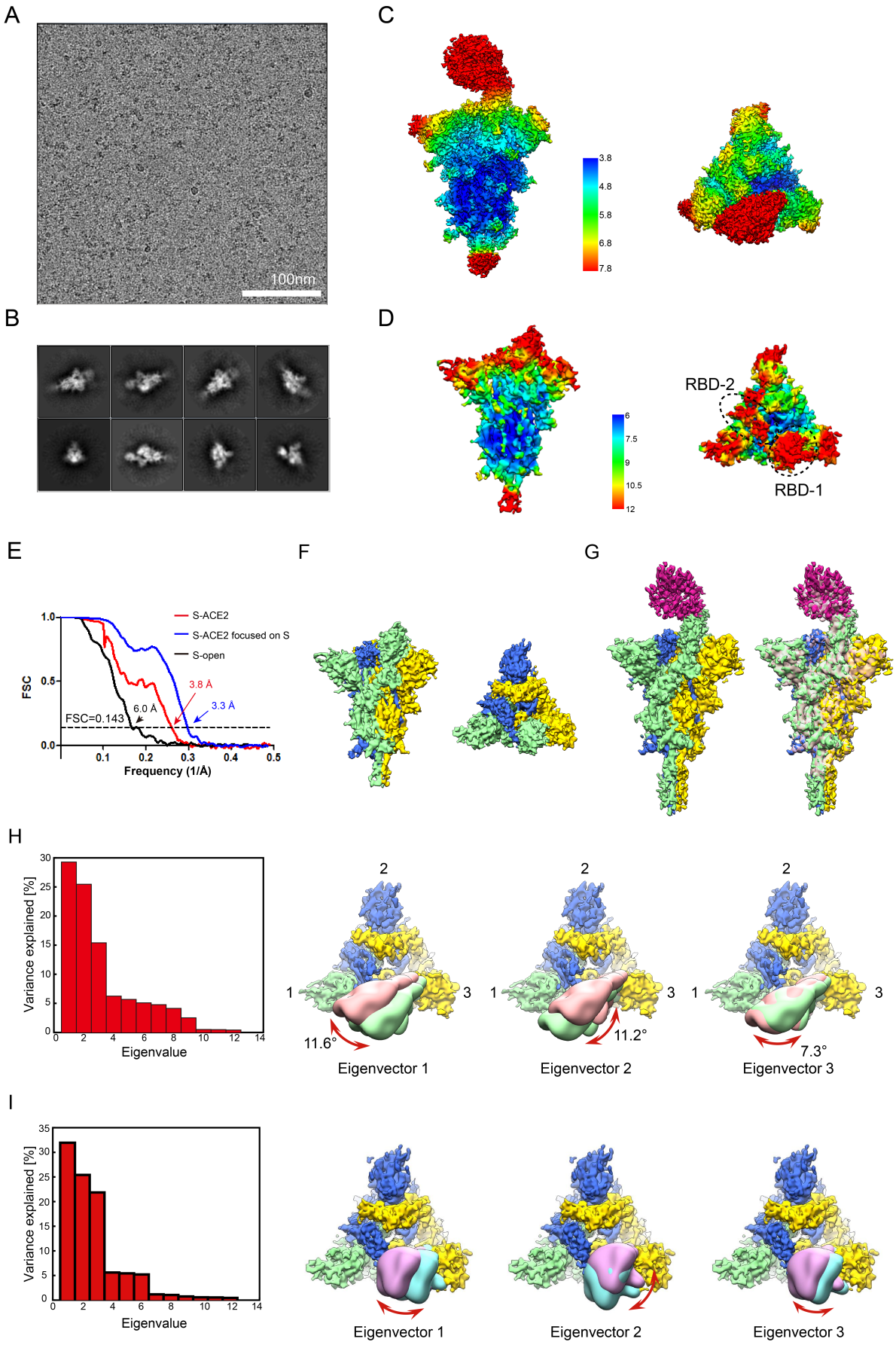
A
100nm
B
C
3.8
4.8
5.8
6.8
7.8
D
6
7.5
9
10.5
12
RBD-2
RBD-1
E
S-ACE2
S-ACE2 focused on S
S-open
FSC
1.0
0.5
0.0
3.8 Å
3.3 Å
6.0 Å
FSC=0.143
0.1
0.2
0.3
0.4
0.5
Frequency (1/Å)
F
G
H
Variance explained [%]
Eigenvalue
1
2
3
11.6°
11.2°
7.3°
Eigenvector 1
Eigenvector 2
Eigenvector 3
I
Variance explained [%]
Eigenvalue
Eigenvector 1
Eigenvector 2
Eigenvector 3

Fig. S5. Cryo-EM analysis on the S-ACE2 complex. (A) Representative cryo-EM image of the S trimer in the presence of ACE2. (B) Reference-free 2D class averages of the sample. (C-D) Local resolution evaluation of the S-ACE2 map (C) and S-open map (D). (E) Resolution assessment of the cryo-EM reconstructions by Fourier shell correlation (FSC) at 0.143 criterion. (F) Unliganded S-open cryo-EM map obtained from this dataset. (G) Cryo-EM map of S-ACE2 complex without cross linker (left, colored), and its overlay with S-ACE2 map with cross linker (pink, low pass filtered to similar resolution, right panel), suggesting they are in similar conformation. (H) Motions of S-ACE2 without cross linker. Left, contributions of all eigenvectors to motions of S-ACE2; right three panels, top view of the map showing the three swing motions along the first 3 eigenvectors. (I) Conformational dynamics of the up RBD in S-open state. Left, contributions of all eigenvectors to motions of S-open. Right three panels, top view of the map showing the three swing motions of the first 3 eigenvectors.

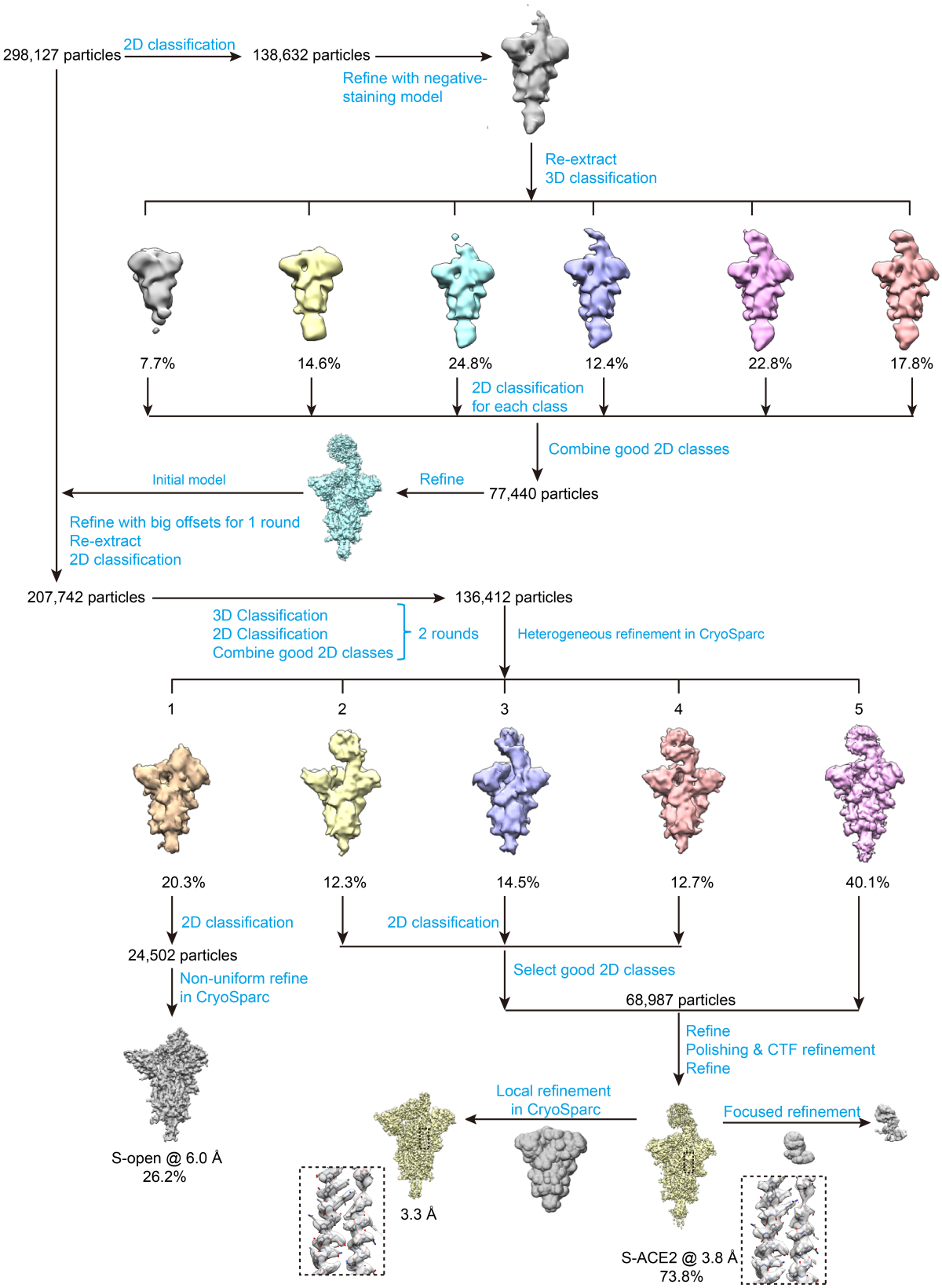

Fig. S6. Cryo-EM data processing procedure for SARS-CoV-2 S trimer in the presence of ACE2.

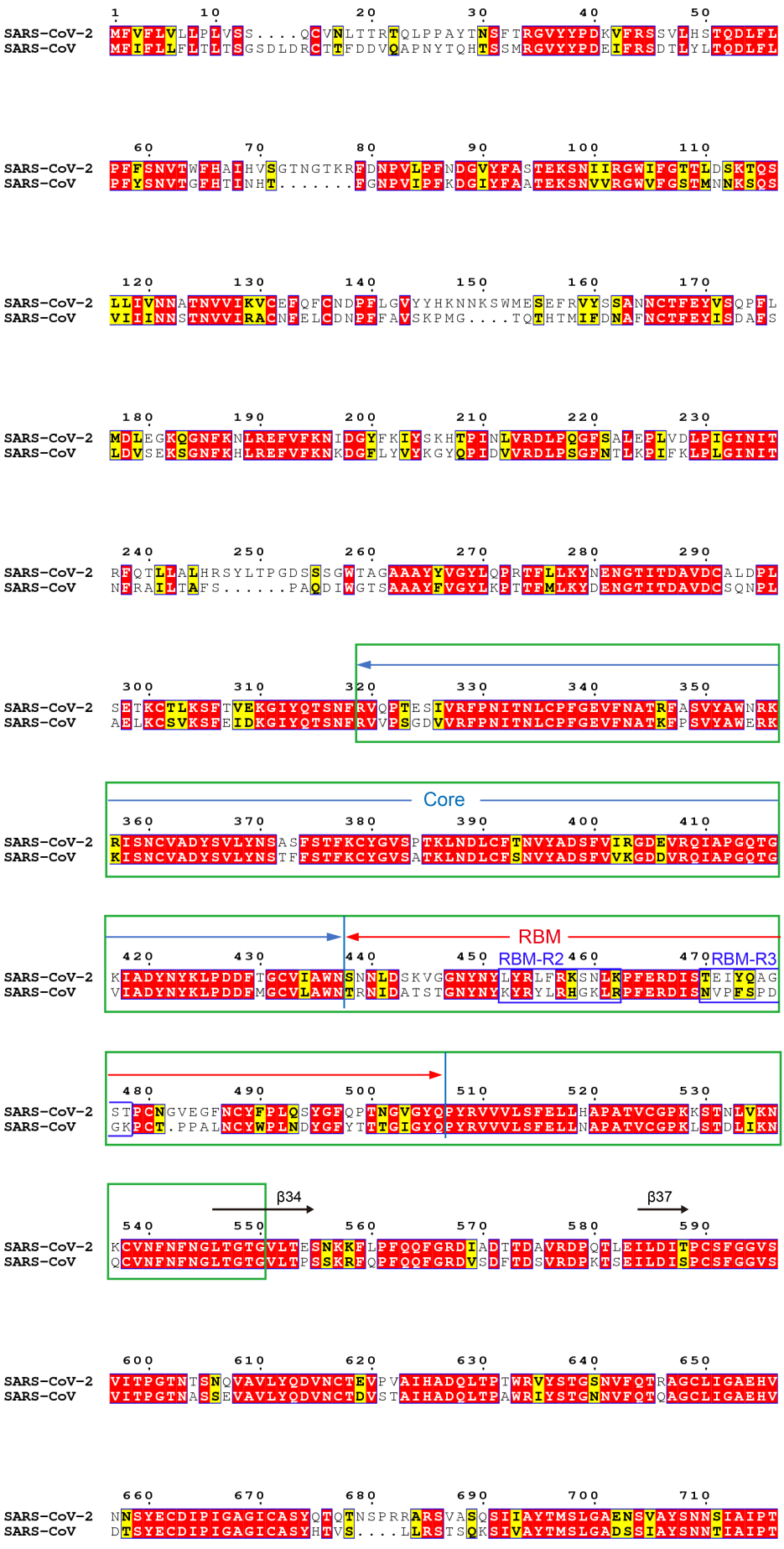
SARS-CoV-2
SARS-CoV
Core
RBM
RBM-R2
RBM-R3
β34
β37

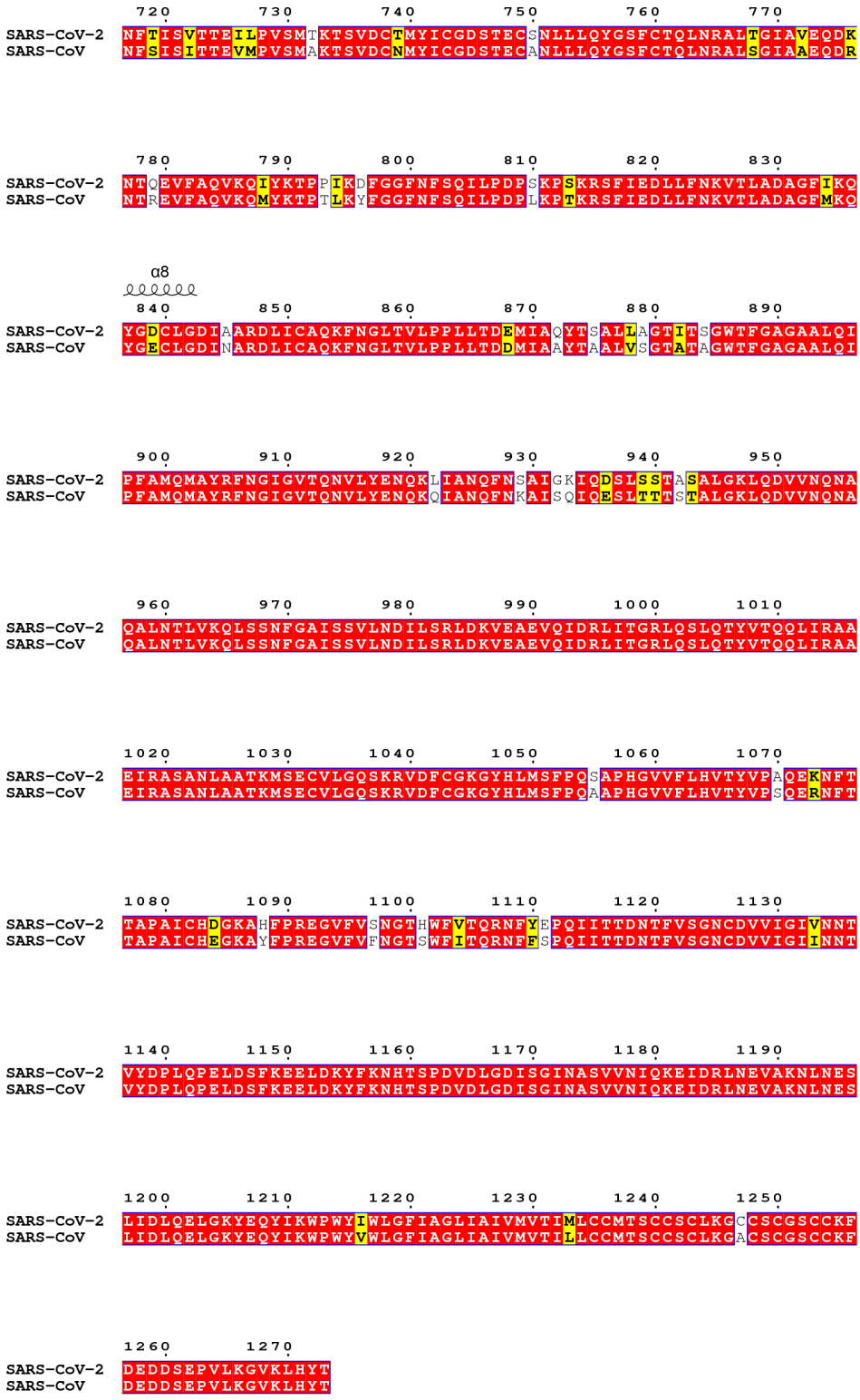

Fig. S7. Amino acid sequence alignment of SARS-CoV-2 S with SARS-CoV S. Sequence alignment was performed by ESPript (*64*). The RBD domain is labeled in green frames, and the subdomains of RBM as well as several other key structural elements are also labeled.

Table S1 Cryo-EM data collection and refinement statistics.

	SARS-CoV-2 S	SARS-CoV-2 S + ACE2 (with cross-linker)		SARS-CoV-2 S + ACE2 (w/o cross-liker)
Data collection				
EM equipment	Titan Krios	Titan Krios		Titan Krios
Voltage (kV)	300	300		300
Detector	K2 Summit	K2 Summit		K2 Summit
Pixel size (Å)	1.02	1.02		1.02
Electron dose ($e^-/Å^2$)	50	50		50
Exposure time (s)	6.45	6.45		6.45
Frames	43	43		43
Defocus range (μm)	-1.0 to -2.4	-1.0 to -2.4		-1.0 to -2.4
Reconstruction				
Softwares		Relion 3.1 & CryoSparc		
Structures	S-closed	S-ACE2	S-open	S-ACE2 (w/o linker)
Final particles	142,345	68,987	24,502	32,866
Symmetry	C3	C1	C1	C1
Final overall resolution (Å)	2.7	3.8	6.0	5.3
Atomic modeling				
Softwares	Swiss-model, Modeller, Phenix, COOT	Phenix, Rosetta, COOT	Rosetta	
Rms deviations				
Bond length (Å)	0.0041	0.0035	0.0081	
Bond Angle (°)	0.97	0.91	1.00	
Ramachandran plot statistics (%)				
Ramachandran favored	94.56%	95.85%	96.62%	
Ramachandran allowed	5.35%	4.10%	3.32%	
Ramachandran outliers	0.09%	0.05%	0.06%	
Molprobity score	2.07	1.78	1.04	
Clash score	15.50	9.35	1.12	
EMRinger score	3.05	1.16		

Table S2 Fusion peptide D828-F855 region involved interactions

D828-F855 region (FP)		Other motifs			Interaction	Distance(Å)
Residue	Atom	Residue	Atom	Location		
K835	N	D614	OD1	SD2 (prot 1)	H-bond	3.74
Y837	N	D614	O	SD2 (prot 1)	H-bond	3.89
Y837	OH	P589	O	SD2 (prot 1)	H-bond	3.56
K854	NZ	D614	OD2	SD2 (prot 1)	Salt bridge /H-bond	2.67
K854	NZ	D614	OD1	SD2 (prot 1)	Salt bridge	3.18
Q836	OE1	N616	N	SD2 (prot 1)	H-bond	3.00
Q853	NE2	A956	O	HR1 (prot 3)	H-bond	3.84
Q853	NE2	N960	OD1	HR1 (prot 3)	H-bond	2.35

Table S3 SARS-CoV-2 S-ACE2 structure revealed RBD-ACE2 interactions

H-bonds at the RBD-ACE2 interface within the S-ACE2 complex

RBD from SARS-CoV-2 S		ACE2		Interaction	Distance(Å)
Residue	Atom	Residue	Atom		
G446	O	Q42	NE2	H-bond	3.49
A475	O	S19	N	H-bond	2.43
N487	OD1	Y83	OH	H-bond	2.26
Y489	OH	Y83	OH	H-bond	3.72
S494	O	H84	NE2	H-bond	2.42
T500	OG1	Y41	OH	H-bond	2.45
G502	N	K353	O	H-bond	2.44
Y505	OH	A386	O	H-bond	2.36
Y505	OH	R393	NH2	H-bond	2.43

Contacting residues at the SARS-CoV-2 RBD-ACE2 interface (distance cutoff of 4 Å)

SARS-CoV-2 S RBD	ACE2
Y453	H34
L455	K31
F456	T27, D30, K31
Y473	T27
A475	S19, T27
G476	S19, Q24
F486	L79, M82, Y83
N487	Q24, Y83
Y489	T27, F28, K31
F490	K31
Q493	K31, H34
S494	H34
Y495	H34
G496	K353
Q498	Y41
T500	Y41, D355, R357
N501	K353
G502	K353, G354
Y505	K353, G354, A386, R393